Major contribution of sarcoplasmic reticulum Ca^{2+} depletion during long-lasting activation of skeletal muscle

Gaëlle Robin[1,2] and Bruno Allard[1,2]

[1]Centre National de la Recherche Scientifique UMR 5534, Centre de Génétique et de Physiologie Moléculaires et Cellulaires, Université Lyon 1, 69622 Villeurbanne, France
[2]Université de Lyon, 69361 Lyon, France

Depolarization of skeletal muscle fibers induces sarcoplasmic reticulum (SR) Ca^{2+} release and contraction that progressively decline while depolarization is maintained. Voltage-dependent inactivation of SR Ca^{2+} release channels and SR Ca^{2+} depletion are the two processes proposed to explain the decline of SR Ca^{2+} release during long-lasting depolarizations. However, the relative contribution of these processes, especially under physiological conditions of activation, is not clearly established. Using Fura-2 and Fluo-5N to monitor cytosolic and SR Ca^{2+} changes, respectively, in voltage-controlled mouse muscle fibers, we show that 2-min conditioning depolarizations reduce voltage-activated cytosolic Ca^{2+} signals with a $V_{1/2}$ of −53 mV but also induce SR Ca^{2+} depletion that decreased the releasable pool of Ca^{2+} with the same voltage sensitivity. In contrast, measurement of SR Ca^{2+} changes indicated that SR Ca^{2+} release channels were inactivated after SR had been depleted and in response to much higher depolarizations with a $V_{1/2}$ of −13 mV. In response to trains of action potentials, cytosolic Ca^{2+} signals decayed with time, whereas SR Ca^{2+} changes remained stable over 1-min stimulation, demonstrating that SR Ca^{2+} depletion is exclusively responsible for the decline of SR Ca^{2+} release under physiological conditions of excitation. These results suggest that previous studies using steady-state inactivation protocols to investigate the voltage dependence of Ca^{2+} release inactivation in fact probed the voltage dependence of SR Ca^{2+} depletion, and that SR Ca^{2+} depletion is the only process that leads to Ca^{2+} release decline during continuous stimulation of skeletal muscle.

The Journal of General Physiology

INTRODUCTION

Depolarization of skeletal muscle fiber induces the release of Ca^{2+} ions from the SR through RyR Ca^{2+} release channels, which in turn activate contraction. Activity of the RyR is a tightly voltage-controlled process that involves the dihydropyridine receptors (DHPRs) anchored in the t-tubules, which act as voltage sensors and transduce membrane potential change into RyR opening (Ríos and Pizarro, 1991; Schneider, 1994; Melzer et al., 1995). The increase in cytosolic Ca^{2+} and development of force that ensue are transient in twitch muscle fibers while the membrane depolarization is maintained, and the progressive decay in Ca^{2+} release during continuous stimulation has been proposed as one of the mechanisms leading to muscle fatigue (Allen et al., 2008). Different mechanisms have been put forward to explain the cytosolic Ca^{2+} decline during maintained depolarization: (a) RyR activity may be inhibited by high cytosolic Ca^{2+} concentrations that are likely to be reached in the proximity of the outer cytoplasmic mouth of the channel during voltage-evoked SR Ca^{2+} release; (b) RyRs may enter a voltage-induced closed inactivated state driven by the DHPR; (c) SR Ca^{2+} efflux may lead to a progressive depletion of SR Ca^{2+}. In frog skeletal muscle, it was demonstrated that Ca^{2+}-dependent inactivation of the flux rate of Ca^{2+} release occurs within tens of milliseconds (Schneider and Simon, 1988; Simon et al., 1991), whereas voltage-dependent inactivation of Ca^{2+} release and SR Ca^{2+} depletion take place later on a slower time scale (Schneider et al., 1987; Brum et al., 1988). In adult mammalian skeletal muscle, early experiments have shown that fibers enter a voltage-dependent inactivated state of contractile refractoriness a few seconds after a K^+ contracture has been elicited (Chua and Dulhunty, 1988). The voltage dependence of inactivation of Ca^{2+} release was later assessed by using conditioning depolarizing pulses of increasing amplitude in voltage-clamped mouse muscle fibers (Collet et al., 2004; Ursu et al., 2004). SR Ca^{2+} depletion is thought to precede the voltage-induced inactivation of RyRs, and a few hundreds of milliseconds appear to be sufficient to cause a reduction of SR Ca^{2+} to a stabilized level (Ursu et al., 2005; Royer et al., 2008). More recently, simultaneous measurements of Ca^{2+} changes inside the SR and in the cytosol under voltage clamp indicated that prolonged Ca^{2+} release results in major SR depletion, which is accompanied by a reduction in SR permeability during Ca^{2+} release (Sztretye et al., 2011).

Correspondence to Bruno Allard: bruno.allard@univ-lyon1.fr
Abbreviation used in this paper: DHPR, dihydropyridine receptor.

The Rockefeller University Press $30.00
J. Gen. Physiol. Vol. 141 No. 5 557–565
www.jgp.org/cgi/doi/10.1085/jgp.201310957

The contributions of voltage-dependent inactivation of Ca^{2+} release and SR Ca^{2+} depletion during long-lasting, voltage-evoked cytosolic Ca^{2+} transients have been mainly investigated by applying conditioning depolarizations of variable amplitudes and durations. However, the measurement of Ca^{2+} changes in the cytosol did not allow to determine whether the alteration of Ca^{2+} transients resulted from SR depletion or voltage-dependent inactivation of Ca^{2+} release channels provoked by the conditioning depolarization. Yet, in a previous study, by measuring Ca^{2+} changes inside the SR in voltage-controlled mouse muscle fibers, we showed that depolarizing steps of very small amplitude from a holding potential of −80 mV induced a slow but substantial SR Ca^{2+} depletion resulting from voltage-induced opening of Ca^{2+} release channels that may not be detected by measuring cytosolic Ca^{2+} changes (Robin and Allard, 2012). Consequently, conditioning depolarizations that apparently did not give rise to a detectable change in cytosolic Ca^{2+} may, however, be responsible for SR depletion and subsequent inhibition of Ca^{2+} transient, which could be misinterpreted as voltage-dependent inactivation.

In this study, we took advantage of the use of the SR Ca^{2+} indicator Fluo-5N in voltage-clamped mouse muscle fibers to investigate the role of SR Ca^{2+} depletion and inactivation of Ca^{2+} release channels in the decline of long-lasting, voltage-evoked Ca^{2+} signals. We showed that conditioning depolarizations at voltages more negative than voltages for which voltage-dependent inactivation occurs produce SR depletion that reduces the pool of releasable Ca^{2+}. Additionally, SR Ca^{2+} signals evoked by trains of action potentials gave evidence of a pronounced SR depletion with no sign of voltage-dependent inactivation, whereas cytosolic Ca^{2+} signals markedly declined during stimulation. These results suggest that SR Ca^{2+} depletion predominantly contributes to the decline of SR Ca^{2+} release during long-lasting depolarizations in skeletal muscle fibers.

MATERIALS AND METHODS

Preparation of skeletal muscle fibers

All experiments were performed in accordance with the guidelines of the French Ministry of Agriculture (87/848) and of the European Community (86/609/EEC). Male OF1 mice were killed by cervical dislocation before removal of flexor digitorum brevis muscles. Single fibers were isolated by a 50-min enzymatic treatment at 37°C using Tyrode's solution containing 2 mg/ml collagenase type I (Sigma-Aldrich).

Electrophysiology

The major part of a single fiber was electrically insulated with silicone grease, and a micropipette was inserted into the fiber through the silicone layer to voltage clamp or current clamp the portion of the fiber free of grease (50–100-µm length) using a patch-clamp amplifier (RK-400; Bio-Logic) in whole-cell configuration (Collet et al., 2004; Robin et al., 2012). Command voltage or current generation and data acquisition were done using the pClamp10 software (Molecular Devices) driving an A/D converter (Digidata 1400A; Molecular Devices). Analogue compensation was systematically used to decrease the effective series resistance. The tip of the micropipette was then crushed into the dish bottom to allow intracellular dialysis of the fiber with the intra-pipette solution (Robin et al., 2012).

Measurements of cytosolic Ca^{2+} using Fura-2

Cells were dialyzed through the micropipette for 20 min using an intracellular solution containing 200 µM Fura-2. Fluorescence was measured on an inverted epifluorescence microscope (Diaphot; Nikon), allowing the detection of fluorescence above 510 nm using a 40× oil-immersion objective. Fluorescence was produced from a 75-W xenon lamp by using a monochromator (Polychrome II; Till Photonics), allowing a 50-Hz alternation of the 340- and 380-nm excitation wavelengths conducted with an optical fiber. Images from a circular region of interest of 450 $µm^2$ corresponding to 12,000 pixels centered on the silicone-free cell portion under study (Fig. S1) were captured with a charge-coupled device camera (CoolSNAP$_{EZ}$; Roper Scientific), and image acquisition and processing were performed using an imaging workbench (MetaFluor; Molecular Devices). Time of exposure ranged between 15 and 50 ms depending on the level of fluorescence obtained after dye loading in each fiber. Background fluorescence at both excitation wavelengths was measured from an equivalent area next to each fiber tested and was subtracted, and the ratio F340/F380 was calculated. The frequency of images captured is indicated in the figure legends.

Measurements of Ca^{2+} in SR lumen using Fluo-5N

Fibers were incubated in Tyrode's solution containing 10 µM Fluo-5N-AM at room temperature for 2 h to allow entry of the dye into the SR and subsequent deesterification. Cells were then dialyzed for 20 min through the micropipette used for clamping, with an internal solution containing 50 mM EGTA to prevent possible contraction during imaging and to avoid contribution of cytosolic Ca^{2+} changes to SR Ca^{2+} signals. Fluo-5N fluorescence was measured using the same setup and experimental conditions that were used for Fura-2 experiments, except that a single excitation wavelength of 488 nm was selected and 4 × 4–pixel binning was used to increase emission light intensity. Time of exposure ranged between 40 and 70 ms depending on the level of fluorescence obtained after dye loading in each fiber. For each voltage pulse, changes in SR Ca^{2+} content were expressed as F/F_0 after background subtraction, where F_0 is the measured fluorescence at the steady state before applying voltage pulses. The frequency of images captured is indicated in the figure legends.

Solutions

The external solution contained, except for Fig. 6 (A and B) (mM), 140 TEA-methanesulfonate, 2.5 $CaCl_2$, 1 $MgCl_2$, and 10 HEPES, adjusted to pH 7.2 with TEA-OH. The Tyrode's solution (Fig. 6, A and B) contained (mM) 140 NaCl, 5 KCl, 2.5 $CaCl_2$, 1 $MgCl_2$, and 10 HEPES, adjusted to pH 7.2 with NaOH. The intra-pipette solution contained (mM) 50 EGTA-KOH, 50 K-glutamate, 5 Na_2-ATP, 5 Na_2-phosphocreatine, 5.5 $MgCl_2$, 5 glucose, and 5 HEPES, adjusted to pH 7.2 with KOH. Stock solutions of Fluo-5N AM and Fura-2 were dissolved at 1 mM in dimethylsulfoxide and 10 mM in water, respectively. Experiments were performed at room temperature.

Statistics

Fits were performed with Microcal Origin (Microcal Software, Inc.). Data are given as means ± SEM.

Online supplemental material

Fig. S1 shows a fluorescence image of a voltage-clamped fiber loaded with Fura-2 and the regions of interest selected for measuring the changes in fluorescence. It is available at http://www.jgp.org/cgi/content/full/jgp.201310957/DC1.

RESULTS

Fig. 1 A shows the cytosolic Fura-2 Ca^{2+} signals produced by long-lasting depolarizing pulses of 50-s duration and of increasing amplitudes. Although the low frequency of Ca^{2+} image capture led to an important underestimation of the early peak of Ca^{2+} signal, we observed that the maximal value of the Ca^{2+} signal increased with the amplitude of the depolarization, giving rise to the classical S-shape voltage-dependent activation curve of SR Ca^{2+} release, relating the peak Ca^{2+} values to voltages. Fig. 1 A also shows that Ca^{2+} signals remained fairly stable for low depolarizing pulses but declined faster and faster during the voltage pulse as depolarization amplitude increased. In all the fibers tested and for each depolarizing pulse, the level of the Ca^{2+} signal at the pulse end was measured and normalized to the peak values, and these ratios were plotted as a function of voltage (Fig. 1 B). Decline in the Ca^{2+} signal was variable at −40 mV; among the eight cells tested, four did not display any decline, as illustrated by the data presented in Fig. 1 A, whereas a decline ranging from 25 to 42% was observed in the four other fibers. Fitting the global relationship with a Boltzmann equation in each cell indicated a mean voltage value inducing half-maximal decline of −13 ± 1.4 mV and a mean steepness factor of 12 ± 1.6 mV. However, meticulous examination of the relationship revealed that for voltages more negative than −20 mV, the Ca^{2+} signal decline tends to display a more negative voltage dependence than the one observed for higher depolarizations, suggesting that two distinct processes with different voltage dependences may contribute to the Ca^{2+} decline. We hypothesized that the increase of the rate of Ca^{2+} signal decline with depolarization could result from voltage-dependent inactivation of Ca^{2+} release channels and/or from SR Ca^{2+} depletion, two processes that may display distinct voltage dependence. To further examine the involvement of these two phenomena in these long-lasting Ca^{2+} signals, we next challenged fibers with very long conditioning pulses of increasing amplitudes.

Fig. 2 A presents the cytosolic Fura-2 Ca^{2+} signals elicited by depolarizing test pulses of 1-s duration to +20 mV, preceded by 2-min conditioning pulses of increasing amplitudes. Here again, the low sampling frequency impeded the measurement of the peak value of the Ca^{2+} signal during the test pulse. We thus took the first data point 1 s after the onset of the test pulse as an index of the maximal Ca^{2+} level reached during the test pulse. Conditioning pulses to voltages as low as −60 mV, which did not evoke any detectable change in cytosolic Ca^{2+}, induced a reduction of the Ca^{2+} transient elicited during the test pulse. As expected, further increases in the amplitude of the conditioning depolarization led to the development of a Ca^{2+} signal of increasing amplitude during the prepulse, which was followed by a more and more reduced Ca^{2+} transient during the test pulse. The peak value of the Ca^{2+} signal during the test pulse was measured in all fibers tested, normalized to the value obtained from a holding potential of −80 mV, and mean values were plotted as a function of the conditioning pulse voltage (Fig. 2 B). Fitting the relationship with a Boltzmann equation in each cell indicated a mean conditioning voltage value inducing half-maximal reduction of −53 ± 2 mV and a mean steepness factor of 6 ± 1.7 mV. These experiments thus confirm that long-lasting depolarizations turn on a voltage-dependent process leading to reduction of Ca^{2+} release, which at this step could not be identified as voltage-dependent inactivation of Ca^{2+} release channels or as SR Ca^{2+} depletion, but exhibiting a very negative voltage dependence that may explain the apparent shift toward negative voltages of the left part of the relationship in Fig. 1 B.

To determine whether voltage-dependent inactivation of Ca^{2+} release channels or SR Ca^{2+} depletion predominates at low voltages, we performed a series of

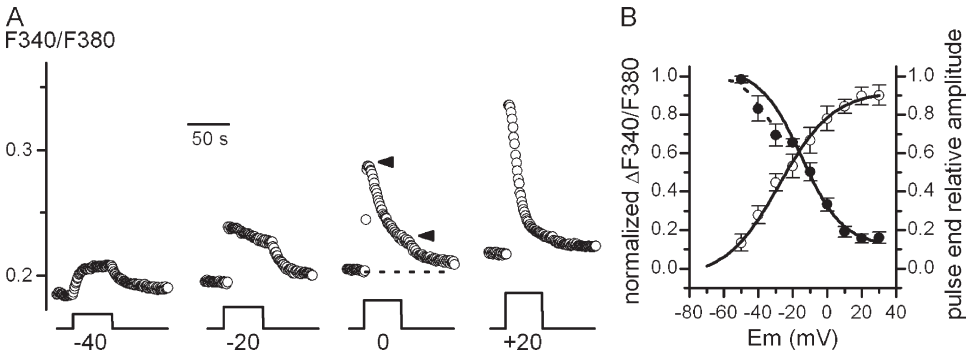

Figure 1. Cytosolic Ca^{2+} changes induced by long-lasting depolarizations of increasing amplitudes. (A) Cytosolic Ca^{2+} changes monitored with Fura-2 (upper traces) in response to 50-s depolarizing pulses of increasing amplitudes from a holding potential of −80 mV (lower traces) in the same fiber. Voltage pulses were given every 2 min, and the fluorescence images were collected at a frequency of 1 Hz. (B) Relationships between the mean maximal changes in Fura-2 fluorescence and membrane potential (○) and between mean values of pulse end decays of Fura-2 signal (measured between the right arrowhead and the dotted line in the example trace) normalized to maximal Fura-2 fluorescence change (measured between the dotted line and the left arrowhead) and membrane potential ($n = 8$) (●). The solid line relationship was fitted with a Boltzmann equation with $V_{1/2}$ of −15 mV and a slope factor of 12 mV, excluding −40- and −30-mV data points. The dotted line curve linking −50-, −40-, and −30-mV data points was drawn by eye.

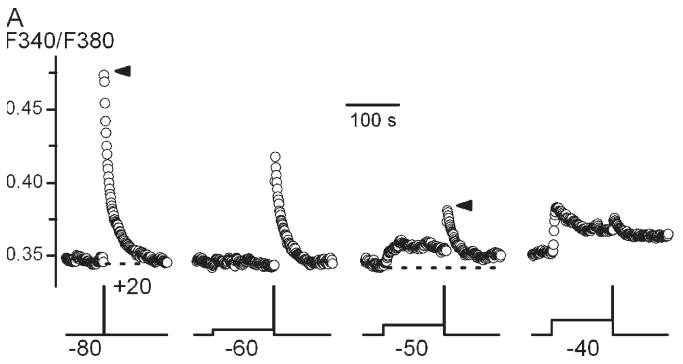

Figure 2. Effect of 2-min conditioning voltage pulses of increasing amplitudes on depolarization-evoked cytosolic Ca^{2+} signals. (A) Cytosolic Ca^{2+} changes monitored with Fura-2 (upper traces) in response to 1-s test pulses to +20 mV after conditioning pulses of increasing amplitudes delivered from a holding potential of −80 mV (lower traces) in the same fiber. Double voltage pulses were given every 2 min, and the fluorescence images were collected at a frequency of 1 Hz. (B) Relationship between the mean maximal changes in Fura-2 fluorescence induced by test pulses (measured between the right arrowhead and the dotted line in the example trace) normalized to the value obtained from a holding potential of −80 mV (measured between the left arrowhead and the dotted line) and conditioning voltages ($n = 6$). The relationship was fitted with a Boltzmann equation with $V_{1/2}$ of −51 mV and a slope factor of 5 mV.

experiments using the SR Ca^{2+} indicator Fluo-5N. We previously showed that long-lasting depolarization led to a decrease in SR Ca^{2+} content caused by Ca^{2+} release followed by a spontaneous recovery phase while depolarization was maintained (Robin et al., 2012). This recovery phase was attributed to voltage-dependent inactivation of Ca^{2+} release channels together with SR Ca^{2+} refilling supported by Ca^{2+}-ATPases. It can yet be considered that sarcolemmal Ca^{2+} influxes should be activated in response to depolarization and in this way might contribute to the time course of recovery of Fluo-5N signals. However, we demonstrated in a previous study that increasing the Ca^{2+} permeability of the sarcolemma using the Ca^{2+} ionophore A23187 in the same experimental conditions did not induce any increase in Fluo-5N fluorescence, indicating that a potentiated sarcolemmal Ca^{2+} influx cannot alter Fluo-5N signals (Robin and Allard, 2012). Fluo-5N is thus very relevant to specifically investigate voltage-dependent inactivation of Ca^{2+} release channels during long-lasting depolarizations. Indeed, in contrast to cytosolic measurement of Ca^{2+} signals in which voltage-dependent inactivation of Ca^{2+} release channels and SR Ca^{2+} depletion both lead to a decline in fluorescence and cannot be distinguished, in Fluo-5N experiments, inactivation of Ca^{2+} release channels gives rise to an increase in Fluo-5N fluorescence, whereas SR depletion gives rise to the opposite. Fig. 3 A shows the Fluo-5N signals induced by long-lasting 50-s depolarizing pulses and of increasing amplitudes. In response to a depolarizing pulse to −30 mV, SR Ca^{2+} content decreased as a result of SR Ca^{2+} release and tended to stabilize at the end of the depolarizing step, strongly suggesting that Ca^{2+} release channels did not inactivate. The absence of a distinct recovery phase cannot however exclude that inactivation occurred but, if it were the case, our data indicate that depletion predominated over inactivation. Higher depolarizations induced faster SR Ca^{2+} content decrease but overall led, before the pulse end, to a Fluo-5N fluorescence recovery phase, the rate of which increased as

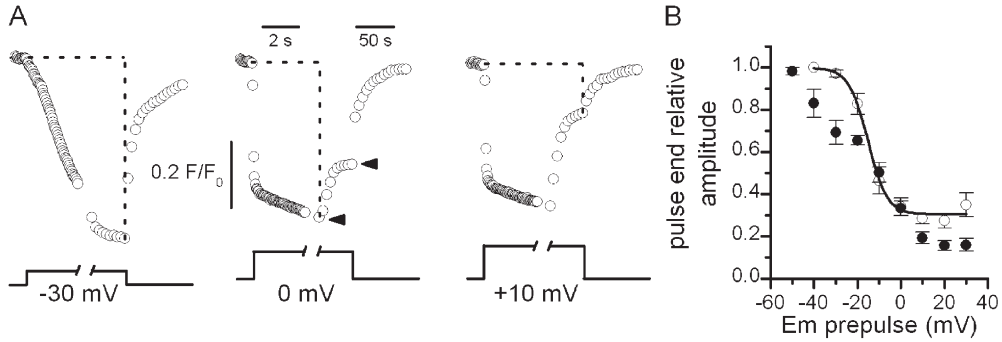

Figure 3. SR Ca^{2+} content changes induced by long-lasting depolarizations of increasing amplitudes. (A) SR Ca^{2+} content changes monitored with Fluo-5N (upper traces) in response to 50-s depolarizing pulses of increasing amplitudes from a holding potential of −80 mV (lower traces) in the same fiber. Voltage pulses were given every 2 min. For each depolarizing pulse, the frequency of fluorescence image capture was 20 Hz until the end of the first second of the pulse, and then it was switched to 0.2 Hz to minimize photobleaching. The time interval between the two sampling frequencies is 5 s. Horizontal and vertical dotted lines indicate the initial level of fluorescence at −80 mV and the time at which the voltage pulse ended, respectively. (B) Relationship between the mean Fluo-5N fluorescence decay at the end of the voltage pulse (measured between the right arrowhead and the dotted line in the example trace) normalized to maximal Fluo-5N fluorescence change during the pulse (measured between the left arrowhead and the dotted line) and membrane potential (○) ($n = 12$). The relationship was fitted with a Boltzmann equation with $V_{1/2}$ of −18 mV and a slope factor of 18 mV. The relationship obtained in Fig. 1 B (●) was superimposed to allow comparison.

depolarization went higher, indicating that Ca^{2+} release channels entered faster and faster the closed inactivated state. Comparable results were obtained when the highest voltages were applied first. As a consequence of inactivation of Ca^{2+} release induced by high voltage pulses, the lower level of cytosolic Ca^{2+} that ensued led to a slowing down of SR reloading upon repolarization. We also observed that for depolarizations to +20 mV, which induced maximal Ca^{2+} release and depletion in less than 1 s (Robin et al., 2012), inactivation occurred in an average of 2.1 ± 0.2 s (n = 6) after the onset of the pulse (not depicted), confirming that depletion precedes inactivation at this voltage. The peak to pulse end recovery of the Fluo-5N signal was measured in all fibers for each depolarizing step, normalized to the peak value of the SR Ca^{2+} drop, and mean values were plotted as a function of voltage (Fig. 3 B). Fitting the relationship with a Boltzmann equation in each cell indicated a mean voltage value inducing half-maximal inactivation of −13 ± 2.1 mV and a mean steepness factor of 4.7 ± 0.4 mV. These experiments likely suggest that during long-lasting depolarizations, voltage-dependent inactivation of Ca^{2+} release channels occurs for high depolarizations with a $V_{1/2}$ of −13 mV, whereas SR Ca^{2+} depletion takes place in response to much lower depolarizations with a $V_{1/2}$ of −53 mV. Along this line, superimposing the relationship between decline of cytosolic Ca^{2+} signals and voltage (Fig. 1 B) on the relationship between rate of recovery of SR Ca^{2+} signals and voltage corroborates that two voltage-dependent processes with distinct voltage sensitivities are responsible for the decline of cytosolic Ca^{2+} signals during long-lasting depolarizations.

To confirm this hypothesis, we next explored the effect of long-lasting conditioning depolarizations of increasing amplitudes on voltage-evoked SR Ca^{2+} signals. We recently demonstrated that SR Ca^{2+} release channels are under the active control of DHPRs at resting membrane potentials so that depolarizing pulses to voltages as low as −60 mV elicit SR Ca^{2+} efflux (Robin and Allard, 2012). Indeed, Fig. 4 A shows that a conditioning depolarizing pulse to −60 mV evoked a slow SR Ca^{2+} efflux that led within the 2-min conditioning pulse to a substantial SR depletion. Consequently, the subsequent test depolarization to +20 mV induced a SR Ca^{2+} decrease caused by active Ca^{2+} release of lower amplitude than the one evoked from a holding potential of −80 mV. Higher conditioning depolarizations to −50 and −40 mV induced more pronounced depletions that led to further reduction of the SR Ca^{2+} decrease produced by the test pulse. The amplitude of the peak SR Ca^{2+} decrease evoked by the test pulse was normalized relative to the total SR Ca^{2+} decrease induced by the conditioning pulse plus the test pulse in each cell for all conditioning pulses, and mean values were plotted as a function of conditioning voltages. Fitting the relationship with a Boltzmann equation in each cell indicated a mean voltage value inducing half-maximal depletion of −51 ± 2 mV and a mean steepness factor of 3.3 ± 0.5 mV (Fig. 4 B). The fact that the voltage dependence of SR depletion induced by conditioning pulses is very close to the voltage dependence of inhibition of cytosolic Ca^{2+} signals induced by long conditioning pulses (−53 mV) likely implies that SR depletion is the predominant process that leads to Ca^{2+} signal decline during long-lasting depolarizations. As expected, when the duration of the conditioning pulse to a given voltage was augmented, the magnitude of SR depletion increased, thereby reducing the SR Ca^{2+} decrease produced by the test pulse. Fig. 5 A illustrates the effects of increasing the duration of a conditioning pulse given to −60 mV. The best fit

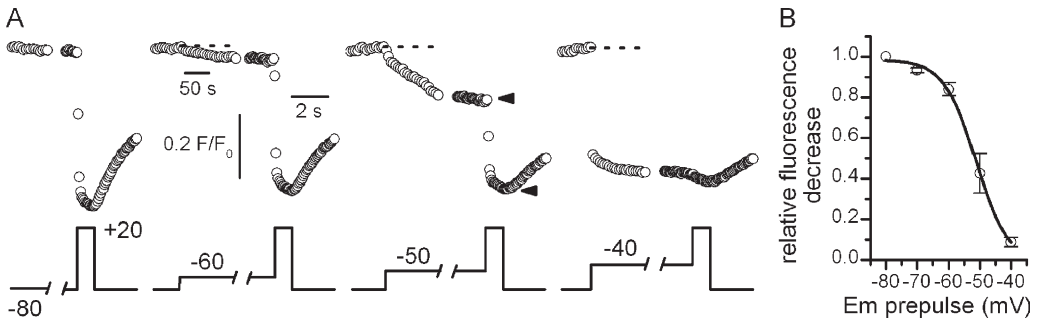

Figure 4. Effect of 2-min conditioning voltage pulses of increasing amplitudes on depolarization-evoked SR Ca^{2+} signals. (A) SR Ca^{2+} content changes monitored with Fluo-5N (upper traces) in response to 1-s test pulses to +20 mV after conditioning pulses of increasing amplitudes delivered from a holding potential of −80 mV (lower traces) in the same fiber. Double voltage pulses were given every 2 min. For each double pulse, the frequency of fluorescence image capture was 0.2 Hz before and during the conditioning pulses, and then it was switched to 15 Hz just before delivering the test pulse. The time interval between the two sampling frequencies is 5 s. (B) Relationship between the mean changes in Fluo-5N fluorescence induced by test pulses (measured between the two arrowheads in the example trace) normalized relative to the total Fluo-5N fluorescence decrease induced by the conditioning pulse plus the test pulse (measured between the right arrowhead and the dotted line) and conditioning voltages (n = 9). The relationship was fitted with a Boltzmann equation with $V_{1/2}$ of −51 mV and a slope factor of 5 mV.

with an exponential function to the relationship between mean values of relative SR Ca^{2+} decrease evoked by the test pulse and duration of the −60-mV conditioning pulse in all cells tested indicated an average time constant of inhibition of 95 s (Fig. 5 B).

In physiological conditions, activation of skeletal muscle Ca^{2+} release is triggered by trains of action potentials. To determine whether the decline of Ca^{2+} signals provoked by SR depletion together with voltage-dependent inactivation of Ca^{2+} release channels in response to long-lasting depolarizations also occurs in response to a train of action potentials, we measured cytosolic and SR Ca^{2+} signals in response to 1-min-long trains of action potentials under current-clamp conditions in the presence of Tyrode's solution. Fig. 6 A shows that cytosolic Fura-2 Ca^{2+} signals declined in average of 55 ± 1% after 1-min trains of action potentials. This decay of Ca^{2+} signals was much less pronounced than the decay displayed by Ca^{2+} signals evoked by a single voltage step to +20 mV because 50 s after the onset of the train of action potentials and 50 s after the onset of the voltage pulse, Ca^{2+} signals had decayed by 52 ± 2% and of 84 ± 2%, respectively. In contrast, Fluo-5N–monitored SR depletion induced by trains of action potentials reached a plateau value without ever recovering during the 1-min-long stimulation in all the cells tested, indicating that voltage-dependent inactivation of Ca^{2+} release does not occur under these conditions of stimulation (Fig. 6 B). These experiments strongly suggest that the decline of the cytosolic Ca^{2+} signal during long-lasting stimulations with trains of action potentials exclusively results from SR depletion. Yet, Fluo-5N experiments under voltage-clamp conditions indicated that inactivation of Ca^{2+} release started to develop in response to voltage pulses around −20 mV (see Fig. 3 B), a potential value far below the one reached by action potentials. We thus hypothesized that the spike depolarization, even reaching high voltage values close to +40 mV, is too short during an action potential for inactivation of Ca^{2+} release to be turned on. To test this hypothesis, we measured SR Ca^{2+} signals in response to a 30-s train of voltage pulses delivered at 50 Hz to +20 mV and lasting 2, 5, 10, and 15 ms. Fig. 6 C shows that in response to trains composed of pulses of 2- and 5-ms duration, the SR signals remained stable until the end of the train, whereas inactivation of Ca^{2+} release started to develop for 10-ms pulses and reinforced for 15-ms pulses and the single 30-s depolarizing step. The lengthening of pulse duration also gave rise to an increase in the rate of SR Ca^{2+} decrease, suggesting an enhancement of the kinetic of Ca^{2+} release. Comparable results were obtained when the longest voltage pulses were applied first. Plotting the peak to train end recovery of the Fluo-5N signal measured in all fibers tested and normalized to the peak value of the SR Ca^{2+} drop as a function of pulse duration indicated that Ca^{2+} release inactivated to an extent equal to half of the inactivation obtained with a single 30-s depolarizing pulse for pulses of 16.2 ± 0.5–ms mean duration (Fig. 6 D).

DISCUSSION

SR Ca^{2+} depletion, Ca^{2+}-dependent inactivation of Ca^{2+} release channels, and voltage-dependent inactivation of voltage sensors are the three mechanisms that have been put forward to produce the decline of Ca^{2+} signals and of force, as a consequence, during continuous stimulation, whereas store-operated, voltage-gated, or excitation-coupled Ca^{2+} influxes, which are possibly activated during stimulation of long duration, might contribute to favor force recovery (Melzer et al., 1995; Berbey and Allard, 2009; Launikonis et al., 2010). In this study, our experimental conditions allowed us to preclude the possible involvement of sarcolemmal Ca^{2+}

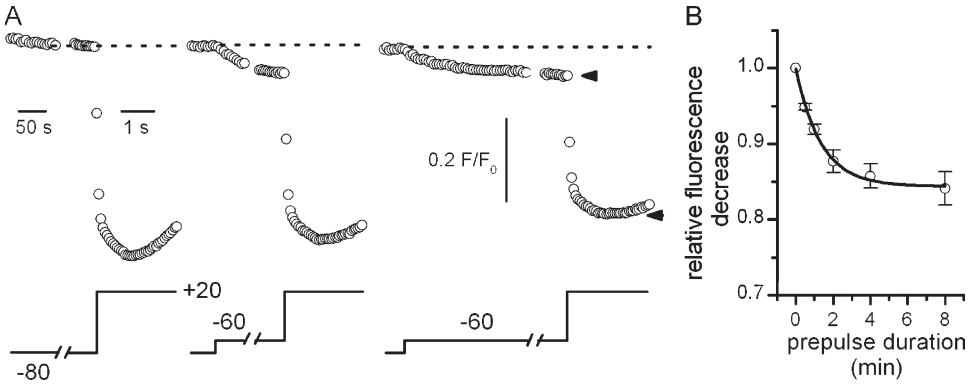

Figure 5. Effect of conditioning depolarizations of increasing duration on depolarization-evoked SR Ca^{2+} signals. (A) SR Ca^{2+} content changes monitored with Fluo-5N (upper traces) in response to 2-s test pulses to +20 mV after conditioning pulses to −60 mV of increasing duration delivered from a holding potential of −80 mV (lower traces) in the same fiber. Double voltage pulses were given every 2 min. For each double pulse, the frequency of fluorescence image capture was 0.2 Hz before and during the conditioning pulses, and then it was switched to 15 Hz just before delivering the test pulse. (B) Relationship between the mean changes in Fluo-5N fluorescence induced by test pulses (measured between the two arrowheads in the example trace) normalized relative to the total Fluo-5N fluorescence decrease induced by the conditioning pulse plus the test pulse (measured between the right arrowhead and the dotted line) and duration of the conditioning pulse (n = 10). The displayed best exponential fit to the mean data indicated a time constant of 95 s.

influx, and our recording conditions with a time scale of over tens of seconds did not offer the required resolution to investigate Ca^{2+}-dependent inactivation that is known to fully develop in a few tens of milliseconds after the onset of depolarization (Schneider and Simon, 1988). These conditions allowed us to focus on SR Ca^{2+} depletion and voltage-dependent inactivation of Ca^{2+} release and to determine to what extent these two processes contribute to the decline of Ca^{2+} signals during long-lasting depolarization of skeletal muscle fibers. By measuring cytosolic Ca^{2+} signals and SR Ca^{2+} changes, we demonstrated that SR Ca^{2+} depletion together with inactivation of Ca^{2+} release channels are involved in the decline of long-lasting, depolarization-evoked Ca^{2+} signals but display different kinetics and voltage dependences. Since the work of Hodgkin and Horowicz (1960), it has been known that prolonged depolarization of muscle fibers causes spontaneous relaxation after contracture, leading to contractile refractoriness. Numerous studies have further demonstrated that this spontaneous relaxation results from an inactivation process that promotes closure of SR Ca^{2+} release channels in a voltage- and time-dependent manner. As we explored in the present study, time and voltage dependence of the inactivation process have been investigated by examining the effects of conditioning pulses on voltage-induced Ca^{2+} or force transients, or indirectly of high K^+ solutions on K^+-induced contractures (Hodgkin and Horowicz, 1960; Lüttgau and Spiecker, 1979; Caputo et al., 1984; Brum et al., 1988; Schnier et al., 1993). These steady-state or double-pulse inactivation protocols revealed that inactivation of Ca^{2+} release requires depolarizations lasting seconds or tens of seconds to develop and is associated with immobilization of intramembrane charge movements, suggesting that inactivation of Ca^{2+} release channels arises from transition of the voltage sensor that controls its opening into an inactivated state (Chandler et al., 1976; Brum and Rios, 1987). In the present study, monitoring SR Ca^{2+} changes under voltage control allowed us to focus on the inactivation

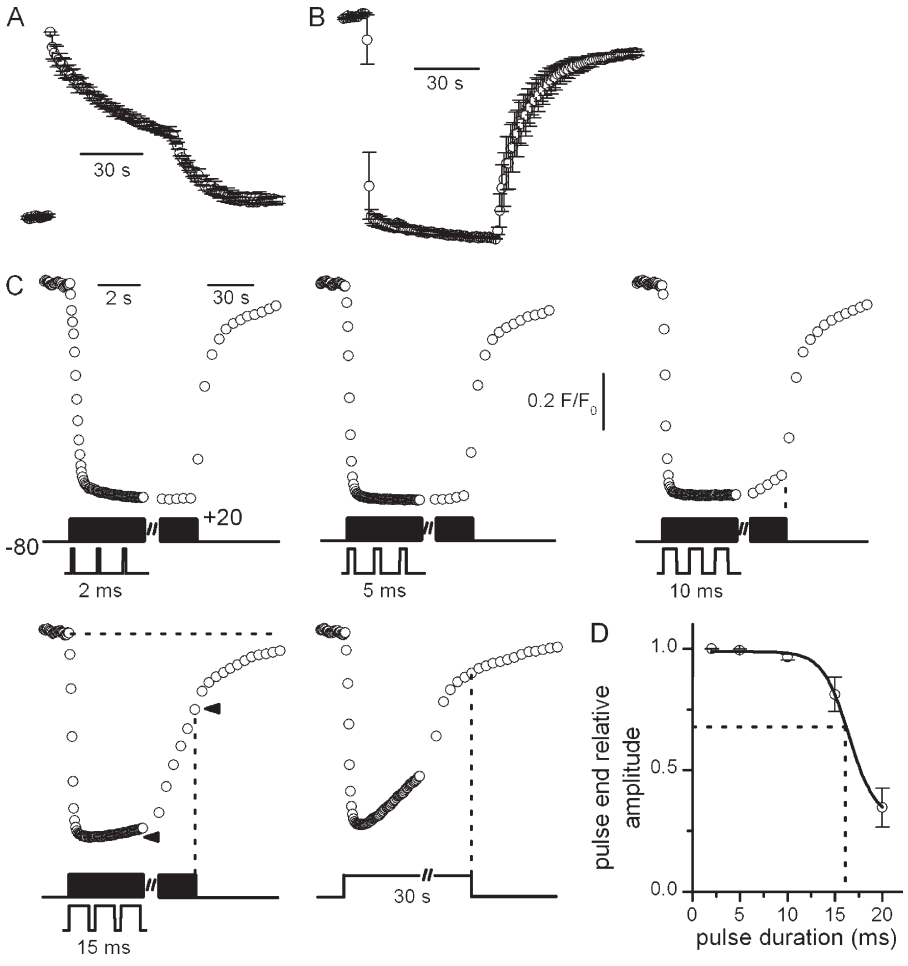

Figure 6. Cytosolic and SR Ca^{2+} decline during long-lasting trains of action potentials or voltage pulses. (A) Means and SEM of cytosolic Ca^{2+} changes monitored with Fura-2 in response to trains of action potentials of 1-min duration induced by bursts of supraliminal current pulses of 0.5-ms duration at a frequency of 50 Hz in current-clamp conditions (n = 3). In each cell, fluorescence values were normalized to the maximal change in fluorescence obtained during the pulse. The frequency of image capture was 1 Hz. (B) Means and SEM of SR Ca^{2+} content changes monitored with Fluo-5N in response to trains of action potentials of 1-min duration obtained in the same conditions as in A (n = 5). In each cell, fluorescence values were normalized to the maximal change in fluorescence obtained during the pulse. Frequency of image capture was 1 Hz. (C) SR Ca^{2+} content changes monitored with Fluo-5N (upper traces) in response to 30-s, 50-Hz trains of voltage pulses of increasing duration delivered to +20 mV from a holding potential of −80 mV (indicated by the middle and lower traces) in the same fiber in voltage-clamp conditions. For each train, the frequency of fluorescence image capture was 20 Hz until the end of the first second of the train, and then it was switched to 0.2 Hz. The time interval between the two sampling frequencies is 5 s. Trains were applied every 2 min. The vertical dotted line indicates the time at which the train ended. (D) Relationship between the mean Fluo-5N fluorescence decay at the end of the train (measured between the right arrowhead and the dotted line in the example trace) normalized to maximal Fluo-5N fluorescence change during the train (measured between the left arrowhead and the horizontal dotted line) and pulse duration (n = 9). The relationship was fitted with a Boltzmann equation with $t_{1/2}$ of 16 ms (indicated by the dotted lines) and a slope factor of 1.4 ms.

process and to demonstrate that inactivation does occur in response to long-lasting depolarizing pulses, but for depolarizations of unexpected high intensity with a $V_{1/2}$ of −13 mV. Early K^+ contracture experiments performed in mammalian skeletal muscle provided a much lower voltage value, producing half-inactivation ($V_{1/2}$) of −52 mV with 3-min conditioning pulses (Chua and Dulhunty, 1988). More recent voltage-clamp studies on mouse muscle fibers indicated a similar $V_{1/2}$ for Ca^{2+} release flux and cytosolic Ca^{2+} transients of −50 and −42 mV using 30 s and stabilized conditioning potential, respectively (Collet et al., 2004; Ursu et al., 2004). These values are very close to the values we obtained in the present study for cytosolic Ca^{2+} signals (−53 mV) as well as for voltage-dependent inhibition of SR Ca^{2+} signals (−51 mV) using 2-min conditioning pulses. However, our SR Ca^{2+} measurements clearly indicated that such low depolarizing conditioning pulses only produced SR Ca^{2+} depletion but were too small to induce inactivation of Ca^{2+} release channels, the voltage dependence of which was found to be 40 mV more positive. This suggests that the voltage-dependent inhibition of K^+ contractures, Ca^{2+} release flux, and transients induced by conditioning pulses in the cited studies did not result from an inactivation process but mainly likely from SR Ca^{2+} depletion at least for low voltages.

The involvement of SR Ca^{2+} depletion in the decline of voltage-evoked Ca^{2+} signals was first established in frog muscle (Schneider et al., 1987). The Ca^{2+} release flux was found to recover from conditioning depolarizing pulses of a few hundred milliseconds at a rate that was dependent on the amount of Ca^{2+} released during the conditioning pulses, demonstrating that SR Ca^{2+} depletion is responsible for the decline of Ca^{2+} signals before Ca^{2+} release channels inactivate. In voltage-clamped mouse muscle fibers, it was further estimated that SR Ca^{2+} content decreased by 80% in response to 100-ms depolarizing pulses above +10 mV (Ursu et al., 2005). More recently, analysis of the evolution of release flux during pulses of longer duration (1–2 s) and simultaneous measurement of cytosolic and luminal SR Ca^{2+} revealed that +30-mV evoked Ca^{2+} release provokes a 65% reduction of the SR Ca^{2+} content and is associated with a decrease in the ability of the SR to empty its Ca^{2+} content (Royer et al., 2008; Sztretye et al., 2011). Our study confirms that depletion precedes inactivation during long-lasting depolarization because inactivation occurred 2.1 s after the onset of the pulse. Overall, our work is the first to provide the voltage dependence of SR Ca^{2+} depletion in parallel with the one of inactivation of Ca^{2+} release in skeletal muscle fibers.

Our findings that SR depletion occurs in response to depolarizations of unforeseen small amplitude that do not provoke inactivation have physiological relevance, especially in the context of sustained muscle activity. Intense muscle exercise leading to fatigue is known to induce considerable electrolyte changes, particularly loss of intracellular K^+ and accumulation of interstitial and tubular K^+ (Sejersted and Sjøgaard, 2000). These K^+ shifts have been shown to lead to a decrease of up to 18 mV of the resting membrane potential in mouse extensor digitorum longus muscle after 1 min of repetitive tetanic stimulation (Juel, 1986). Our study indicates that such changes in the resting membrane potential should produce SR Ca^{2+} depletion, contributing to the decrease of contractile performance. Muscle fatigue caused by SR Ca^{2+} depletion is thus expected to occur not only during muscle activity (see below) but also during resting intervals before recovery of electrolyte changes takes place. Additionally, our results emphasize that the control of internal membrane potential is an absolute prerequisite when investigating Ca^{2+} signaling in skeletal muscle, because uncontrolled changes in the membrane potential even of a few millivolts may produce alteration of the SR Ca^{2+} content that cannot be detected with cytosolic Ca^{2+} indicators and affect in this way the amount of Ca^{2+} released.

In physiological conditions, the excitatory signal consists of a train of action potentials. From frog to human skeletal muscle, it has long been known that the contractile response declines during continuous high frequency stimulation, caused in part by the decline of the Ca^{2+} signal that initiates contraction (Allen et al., 2008). In this study, we showed that the cytosolic Ca^{2+} signal declined during a 1-min train of action potentials, but our SR Ca^{2+} measurements clearly indicated that SR Ca^{2+} depletion was maintained during the entire duration of the stimulation, giving evidence that Ca^{2+} release channels do not close. We concluded from these experiments that the cytosolic Ca^{2+} signal decline during a sustained train of action potentials exclusively arose from SR depletion. The mechanisms involved in the Ca^{2+} signal decline are consequently different when the fiber is stimulated by long-lasting depolarizing pulses of high voltage or by a train of action potentials, as SR Ca^{2+} depletion together with inactivation occurs in the first situation, whereas only SR Ca^{2+} depletion takes place in the second. Comparing the decay of Ca^{2+} signals in response to a train of action potentials (52% after 50 s) and in response to a single voltage pulse to +20 mV (84% after 50 s) led us to estimate that during a voltage step, 52% of the decay may be caused by depletion, whereas 32% may be caused by inactivation. Our last series of experiments gives an explanation for this discrepancy by demonstrating that the depolarization produced by an action potential is likely too short to turn on inactivation processes and should last longer than 10 ms to induce Ca^{2+} release channel closure. These results have important physiological consequences. The physiological excitatory stimulus of muscle fibers, which consists of a train of action potentials, is indeed optimal; the tetanic rate of depolarization induced by a train of

action potentials allows the SR to reach its maximal Ca^{2+} release capacity (Ziman et al., 2010; Robin et al., 2012) but without producing voltage-dependent inactivation of Ca^{2+} release channels. This guarantees that maximal contractile force can be generated. However, in return, SR Ca^{2+} depletion cannot be prevented and should thus predominantly contribute to the decline of Ca^{2+} release and force during long-lasting stimulation of muscle leading to fatigue.

We thank Vincent Jacquemond for critical comments on the manuscript.

This work was supported by grants from the Université Lyon 1, the Centre National de la Recherche Scientifique, and the Association Française contre les Myopathies.

Edward N. Pugh Jr. served as editor.

Submitted: 4 January 2013
Accepted: 18 March 2013

REFERENCES

Allen, D.G., G.D. Lamb, and H. Westerblad. 2008. Skeletal muscle fatigue: cellular mechanisms. *Physiol. Rev.* 88:287–332. http://dx.doi.org/10.1152/physrev.00015.2007

Berbey, C., and B. Allard. 2009. Electrically silent divalent cation entries in resting and active voltage-controlled muscle fibers. *Biophys. J.* 96:2648–2657. http://dx.doi.org/10.1016/j.bpj.2009.01.008

Brum, G., and E. Rios. 1987. Intramembrane charge movement in frog skeletal muscle fibres. Properties of charge 2. *J. Physiol.* 387:489–517.

Brum, G., E. Ríos, and E. Stéfani. 1988. Effects of extracellular calcium on calcium movements of excitation-contraction coupling in frog skeletal muscle fibres. *J. Physiol.* 398:441–473.

Caputo, C., P. Bolaños, and G.F. Gonzalez. 1984. Effect of membrane polarization on contractile threshold and time course of prolonged contractile responses in skeletal muscle fibers. *J. Gen. Physiol.* 84:927–943. http://dx.doi.org/10.1085/jgp.84.6.927

Chandler, W.K., R.F. Rakowski, and M.F. Schneider. 1976. Effects of glycerol treatment and maintained depolarization on charge movement in skeletal muscle. *J. Physiol.* 254:285–316.

Chua, M., and A.F. Dulhunty. 1988. Inactivation of excitation–contraction coupling in rat extensor digitorum longus and soleus muscles. *J. Gen. Physiol.* 91:737–757. http://dx.doi.org/10.1085/jgp.91.5.737

Collet, C., S. Pouvreau, L. Csernoch, B. Allard, and V. Jacquemond. 2004. Calcium signaling in isolated skeletal muscle fibers investigated under "silicone voltage-clamp" conditions. *Cell Biochem. Biophys.* 40:225–236. http://dx.doi.org/10.1385/CBB:40:2:225

Hodgkin, A.L., and P. Horowicz. 1960. Potassium contractures in single muscle fibres. *J. Physiol.* 153:386–403.

Juel, C. 1986. Potassium and sodium shifts during in vitro isometric muscle contraction, and the time course of the ion-gradient recovery. *Pflugers Arch.* 406:458–463. http://dx.doi.org/10.1007/BF00583367

Launikonis, B.S., R.M. Murphy, and J.N. Edwards. 2010. Toward the roles of store-operated Ca^{2+} entry in skeletal muscle. *Pflugers Arch.* 460:813–823. http://dx.doi.org/10.1007/s00424-010-0856-7

Lüttgau, H.C., and W. Spiecker. 1979. The effects of calcium deprivation upon mechanical and electrophysiological parameters in skeletal muscle fibres of the frog. *J. Physiol.* 296:411–429.

Melzer, W., A. Herrmann-Frank, and H.C. Lüttgau. 1995. The role of Ca^{2+} ions in excitation-contraction coupling of skeletal muscle fibres. *Biochim. Biophys. Acta.* 1241:59–116. http://dx.doi.org/10.1016/0304-4157(94)00014-5

Ríos, E., and G. Pizarro. 1991. Voltage sensor of excitation-contraction coupling in skeletal muscle. *Physiol. Rev.* 71:849–908.

Robin, G., and B. Allard. 2012. Dihydropyridine receptors actively control gating of ryanodine receptors in resting mouse skeletal muscle fibres. *J. Physiol.* 590:6027–6036. http://dx.doi.org/10.1113/jphysiol.2012.237321

Robin, G., C. Berthier, and B. Allard. 2012. Sarcoplasmic reticulum Ca^{2+} permeation explored from the lumen side in *mdx* muscle fibers under voltage control. *J. Gen. Physiol.* 139:209–218. http://dx.doi.org/10.1085/jgp.201110738

Royer, L., S. Pouvreau, and E. Ríos. 2008. Evolution and modulation of intracellular calcium release during long-lasting, depleting depolarization in mouse muscle. *J. Physiol.* 586:4609–4629. http://dx.doi.org/10.1113/jphysiol.2008.157990

Schneider, M.F. 1994. Control of calcium release in functioning skeletal muscle fibers. *Annu. Rev. Physiol.* 56:463–484. http://dx.doi.org/10.1146/annurev.ph.56.030194.002335

Schneider, M.F., and B.J. Simon. 1988. Inactivation of calcium release from the sarcoplasmic reticulum in frog skeletal muscle. *J. Physiol.* 405:727–745.

Schneider, M.F., B.J. Simon, and G. Szucs. 1987. Depletion of calcium from the sarcoplasmic reticulum during calcium release in frog skeletal muscle. *J. Physiol.* 392:167–192.

Schnier, A., H.C. Lüttgau, and W. Melzer. 1993. Role of extracellular metal cations in the potential dependence of force inactivation in skeletal muscle fibres. *J. Muscle Res. Cell Motil.* 14:565–572. http://dx.doi.org/10.1007/BF00141553

Sejersted, O.M., and G. Sjøgaard. 2000. Dynamics and consequences of potassium shifts in skeletal muscle and heart during exercise. *Physiol. Rev.* 80:1411–1481.

Simon, B.J., M.G. Klein, and M.F. Schneider. 1991. Calcium dependence of inactivation of calcium release from the sarcoplasmic reticulum in skeletal muscle fibers. *J. Gen. Physiol.* 97:437–471. http://dx.doi.org/10.1085/jgp.97.3.437

Sztretye, M., J. Yi, L. Figueroa, J. Zhou, L. Royer, P. Allen, G. Brum, and E. Ríos. 2011. Measurement of RyR permeability reveals a role of calsequestrin in termination of SR Ca^{2+} release in skeletal muscle. *J. Gen. Physiol.* 138:231–247. http://dx.doi.org/10.1085/jgp.201010592

Ursu, D., R.P. Schuhmeier, M. Freichel, V. Flockerzi, and W. Melzer. 2004. Altered inactivation of Ca^{2+} current and Ca^{2+} release in mouse muscle fibers deficient in the DHP receptor γ_1 subunit. *J. Gen. Physiol.* 124:605–618. http://dx.doi.org/10.1085/jgp.200409168

Ursu, D., R.P. Schuhmeier, and W. Melzer. 2005. Voltage-controlled Ca^{2+} release and entry flux in isolated adult muscle fibres of the mouse. *J. Physiol.* 562:347–365. http://dx.doi.org/10.1113/jphysiol.2004.073882

Ziman, A.P., C.W. Ward, G.G. Rodney, W.J. Lederer, and R.J. Bloch. 2010. Quantitative measurement of Ca^{2+} in the sarcoplasmic reticulum lumen of mammalian skeletal muscle. *Biophys. J.* 99:2705–2714. http://dx.doi.org/10.1016/j.bpj.2010.08.032